Contents lists available at **CEPM**

Journal of Computational Engineering and Physical Modeling

Journal homepage: http://www.jcepm.com/

Use of Tuned Mass Dampers in Controlling the Vibrations of Steel Structures with Vertical Irregularity of Mass

M. Babaei[1*] and A. Moniri[1]

2. Department of Civil Engineering, Faculty of Engineering, University of Zanjan, Zanjan, Iran

Corresponding author: *mbabaei@znu.ac.ir*

http://dx.doi.org/10.22115/CEPM.2018.137303.1035

ARTICLE INFO

Article history:
Received: 11 January 2018
Revised: 14 June 2018
Accepted: 27 June 2018

Keywords:
Optimization,
Irregular Structures,
Tuned Mass Dampers,
Near-Field Earthquake,
Far-Field Earthquake.

ABSTRACT

One of the common methods of the inactively controlling structures subject to earthquakes is the use of Tuned Mass Damping (TMD) systems. These dampers consist of three major parameters, namely mass, damping and stiffness. TMDs generally reduce the response domain by influencing a mode, which is most often the first mode of the structure. Since the TMD parameters remain constant during vibrations, it is very important to tune them correctly and optimally. In this study, a ten-story structural model with mass irregularities has been investigated. The mass ratio for the mass damper is assumed to be at 2%. Considering a nonlinear structure, to tune the frequency of the mass damper to its optimum value, proposed experimental relationships have been used. Both regular and irregular structures have been subjected to seven near-field and far-field earthquakes and amplified dynamic analysis from 0.1g to 1.0g with 0.1g steps and mass dampers has been used to evaluate the structural behavior. Based on the analyses outcomes, it can be seen that the TMD in structures with mass irregularities shows a better performance in the first 5 floors compared to the absence of dampers. In addition, by creating mass irregularities in the floor levels, the structure becomes more prone to damages in near-field earthquakes and the performance of the TMDs is better in earthquakes of far-field nature.

1. Introduction

The use of inactive TMDs is one of the most effective methods of structural control. The concept of mass dampers was initially introduced by Frahm in 1909 to reduce the ship hull vibrations due to sea waves [1]. This damper has a mass of 1-5% of the entire structural weight, which connects to a part of the structure with the largest displacement, via a spring and a damper. When this mode of the structure is stimulated, the damper absorbs and dampens the earthquake energy through its anti-phase movements in relation to the structure. The installation and activation of a mass damper is a simple process. In fact, some industrial appliances within the structure can be used as dampers. Contrary to the other means of structural control, such as active control, the maintenance of mass dampers is not extremely costly.

2. Literature Review

The first successful experiment of using TMDs in seismic loads was performed in 1973 by Wirsching and Yao [2]. It is important to note that the full potential of an active or inactive mass damper can be reached when its parameters are optimized [3]. Most of the researches on optimized design of TMDs use methods based on assumptions made considering parameters such as mass distribution, stiffness and damping of mass dampers as well as the input vibrations. Given the large number of variables in the optimized design of mass dampers, the use of standard optimization techniques requires extensive calculations; therefore, use of experimental methods can be considered acceptable in tuning such dampers. In 1976, Dong [4] introduced a lightweight section of the structure with large displacements as the vibration absorbent.

Ohno et al. in 1977 [5] tuned the optimum frequency of a mass damper such that the sum of the squares of the accelerations of the structure was minimized. They assumed a constant density spectrum for the earthquake acceleration in a given frequency range. Randall et al. [6] used numerical analysis to find the optimum parameters of a linear mass damper for a linearly damping structure. They changed the inherent damping of the structure from 0 to 0.5% and increased the mass ratio of the damper from 0.01 to 0.04. In this study, the regular and irregular structures of Pirizadeh and Shakib [7] are utilized to model and control vibrations and improve the structural behavior.

During the past decade, optimization of steel structures has been carried out to find the best size, shape and topology of the structural systems with optimal weight or maximum displacement [8, 9]. Optimal positioning obtained for braced frames and outrigger-belt truss buildings, where all of the structural systems assumed to be as passive control [10, 11].

The structural modeling is compared and verified against that of the aforementioned research and following successful verification of the 10 storey building model, TMDs will be installed on the structure. The structure will then be subjected to various earthquake types and ultimately, the improved behavior of the structure will be presented in the form of vibration control parameters such as displacement value, structural cross sections and result deviation in comparison to the average value.

3. Case Study

As previously mentioned, the replica used for modeling of regular structures is extracted from Pirizadeh and Shakib [7]. Two-dimensional models with mass regularity and irregularity have been simulated and verified in the OpenSees software. The structure is assumed to be a regular 10 storey steel building with storey heights of 3 meters. The structure is 5 x 5 meters in plan, as shown in Fig. 1. The lateral load bearing system of the structure in both directions consists of a specific bending frame and the roof system is a two-way concrete slab with a rigid diaphragm.

The structure is designed for a high risk seismic area and soil type II, as defined in Standard No. 2800-05 [12] and National Building Code [13]. The uniform dead load on the structure is assumed to be 700 kg/m^2 and the live load on the floors is set at 200 kg/m^2. The beam and column sections of the regular structure are shown in Fig. 1. The primary period of the regular structure is 2.01s with a mass participation of 81%. Three irregular models have also been produced from the regular structure, based on the recommendations of Pirizadeh and Shakib [7], such that in addition to constant inherent damping and mode one period for the structures, the base shear of the regular and irregular structures should remain the same in the linear range. The inherent damping for all structures is set to 2% [7]. The cross sections of the beams and columns agree with those of the regular model.

Considering the two-way symmetry of the structure, only a 2D model has been simulated. In the software, "Uniaxial Material Steel02" is defined as material property and the "Nonlinear Beam Column" is selected for elements type. In order to take the effect of P-Δ into account, the coordinate transformation command of geomTransf P-Delta has been used. To simulate the panel zone, the eight node Krawinkler model has been used [14]. To produce the structures with mass irregularities from the regular structure, based on the Standard No. 2800-05, the mass of the two subsequent stories shall be twice one another; therefore, the coefficients shown in Fig. 2 were used.

The distribution factors of mass for the irregular structure are set as $\beta = 0.995$ for the first floor; $\alpha = 0.87$ for floors 1-5the; and $\lambda = 0.93$ for the 5th floor. The period of the irregular structure for floor 1, floors 1-5 and floor 5 are respectively, 2.013, 2.015 and 2.012, which have been modeled with an engineering error of 0.25. In Fig. 2, m represents the mass of each storey and the irregularity coefficient is determined from Eq. 1.

$$Irregularity\,Coefficient = \frac{Mass\ of\ the\ irregular\ storey}{Mass\ of\ the\ adjacent\ upper\ storey} \tag{1}$$

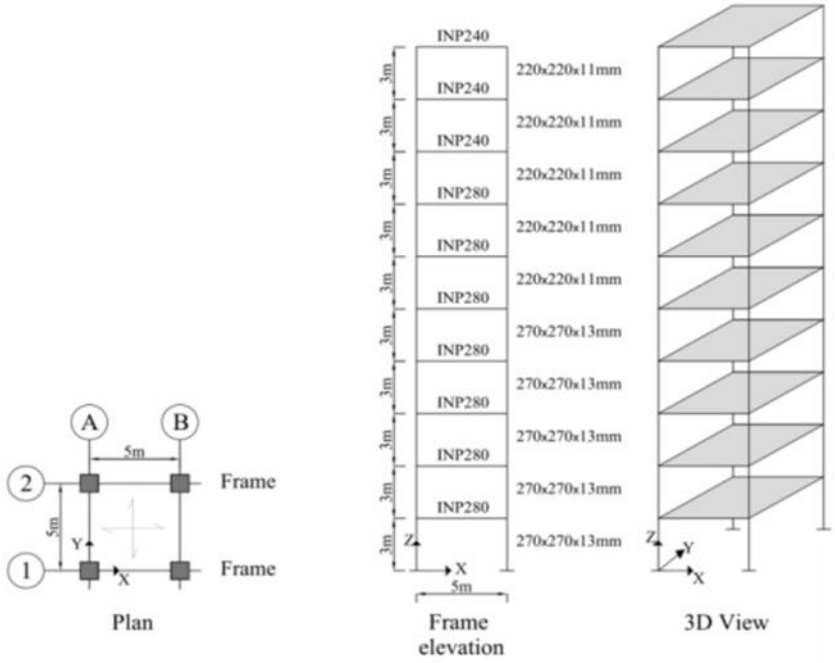

Fig. 1. Two-dimensional and Three-dimensional view of the 10-storey Structure [7].

In order to derive the irregular structures from the regular one, the inherent damping, the first mode period and the elastic base shear of both structures should be the same. At this stage, to ensure creating irregular models based on the regular structure, the elastic base shear of the two models are compared; the mass irregularity curves of the first storey are shown in Fig. 3 as a sample for the 3 irregular models. To verify, the pushover analysis and the curves of regular and irregular structures are compare; based on Fig. 3, the results correlate satisfactorily.

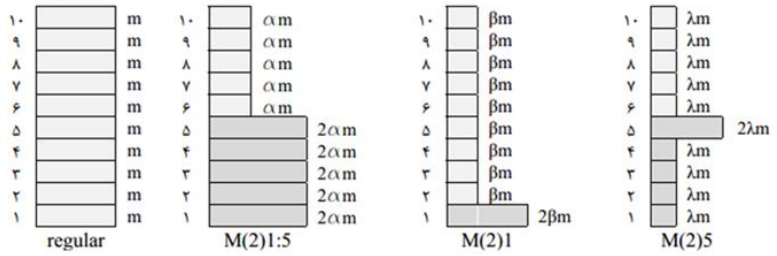

Fig. 2. Assumed Coefficients and Irregularities.

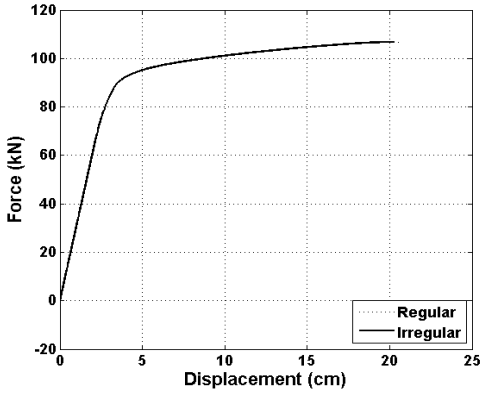

Fig. 3. Regular and Irregular Structural Push Curve for 1st Floor.

4. Tuned Mass Damper

Tuned Mass Damper (TMD) is an inactive control system consisting of 3 mechanical parts: mass, spring and viscous damper. One of its uses is to dampen the vibrations in structures, caused by earthquakes and wind. Hence it is essential to optimally tune the parameters of the TMD. To further explain the performance of a TMD, the parametric relationships for a system with 1 degree of freedom are presented below. Footnote d refers to TMDs.

$$\omega^2 = \frac{k}{m} \tag{2}$$

$$c = 2\xi\omega m \tag{3}$$

$$\omega_d^2 = \frac{k_d}{m_d} \tag{4}$$

$$c_d = 2\xi_d\omega_d m_d \tag{5}$$

$$\bar{m} = \frac{m_d}{m} \tag{6}$$

where, $\bar{m}$ is the mass ratio, ω is the angular frequency of the 1st mode, k is the structural stiffness (N/m), m is the mass (N) and c is damping (N.s/m).

TMDs are installed on the roof of regular and irregular structures. “ZeroLength” elements are used to model the mass damper in both the reference study and the present research. The element consists of an axial spring replicating the damper stiffness and a viscous element for the damping effect of the mass damper. The stiffness and damping values are calculated from the optimum value equations of Pastia and Luca [15] shown in Eq. 7 and 8.

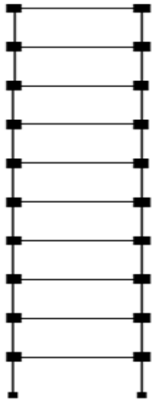

Fig. 4. Software Model.

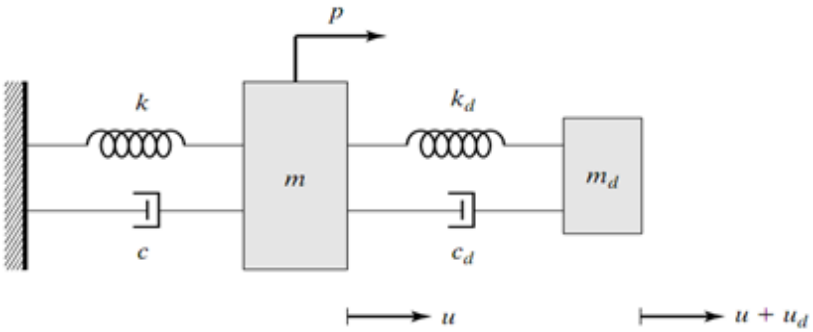

Fig. 5. A system with 1 DOF, Equipped with a TDM.

$$f_{TMD} = \frac{f_1}{1+\mu} \tag{7}$$

$$\xi_{opt} = \sqrt{\frac{3\mu}{8(1+\mu)^3}} \tag{8}$$

where, μ is the mass ratio, f_1 is the first mode frequency, f_{TMD} is the frequency of the TMD and ξ_{opt} is the optimal damping of the TMD.

The simulated earthquakes are selected using the P695FEMA [16] instructions.

Table 1.
Far-Field Earthquakes Applied to the Structures

No.	Earthquake	Station	PGA(g)
1	Northridge	Beverly Hill	0.52
2	Northridge	Canyon Country-WLC	0.48
3	Duzce, Turkey	Bolu	0.82
4	Hector Mine	Hector	0.34
5	Imperial Valley	Delta	0.35
6	Imperial Valley	El Centro Array #11	0.38
7	Kobe, Japan	Nishi-Akashi	0.51

Table 2.
Near-Field Earthquakes Applied to the Structure.

No.	Earthquake	Station	PGA(g)
1	Gazli, USSR	Karakyr	0.71
2	Imperial Valley-06	Bonds Corner	0.76
3	Imperial Valley-06	Chihuahua	0.28
4	Nahanni, Canada	Site 1	1.18
5	Nahanni, Canada	Site 2	0.45
6	Loma Prieta	BRAN	0.64
7	Loma Prieta	Corralitos	0.51

5. Dynamic Analysis

After performing about ten analyses on the simulated structures, in order to facilitate the efficiency evaluation of the control system, specific benchmarks have been assumed as it relates to the vibration behavior of the structure. These benchmarks are of the nature of maximum results and norm results, which will be explained below. In this research for evaluation criteria have been used, two of which relate to the displacements of the structure roof and the other two are concerning the base shear. The following equations, index *c* refers to conditions controlled with mass dampers and index *u* refers to the uncontrolled condition. In addition, *x* defines the displacement of the roof and *v* represents base shear.

The results of the nonlinear dynamic analysis for the Northridge earthquake (an example of a far-field earthquake) and the Loma Prieta earthquake (a near-field example), with maximum accelerations of 0.1 and 0.5 times the gravitational acceleration, are shown in Figures 6 to 9. The rest of the results are also shown in Tables 3 to 6, giving the average value of the outcomes of 7 far-field and 7 near-field earthquakes. Since the analysis results of the first five floors and the mass irregularity of the fifth floor are similar to the results of the mass irregularity of the first floor, therefore, the results have not been displayed to avoid repetition.

Based on the sample Northridge earthquake curves, for regular structures with and without a damper, it can be observed that with the increase in the maximum acceleration, the structures enter the nonlinear zone and the vibration occurs in this zone. Therefore, in higher maximum accelerations, the structure becomes distant from the y=0 axis and begins vibration about the resting zone.

Based on the values of Tables 3 to 6, it can be seen that the result improvement percentage for the maximum displacement of the roof (and the same value for the base shear), decrease with the increasing maximum acceleration of the applied earthquakes. As a result, in addition to the structure becoming nonlinear, which changes the frequency, the earthquake magnitude increases and the controllability of the structural vibrations decrease.

With the structure entering the nonlinear zone, the structural frequency decreases and its period increase, which itself is an important factor in interrupting the controlled frequency of the mass damper. This is due to the fact that TMD is tuned based on the structure's first mode and its value remains constant during the earthquake application; with the structure entering the nonlinear zone, the structural frequency changes, which in return causes the structure and the TMD to have different frequencies and lose the optimally controlled zone. Hence the performance of the mass damper will be reduced.

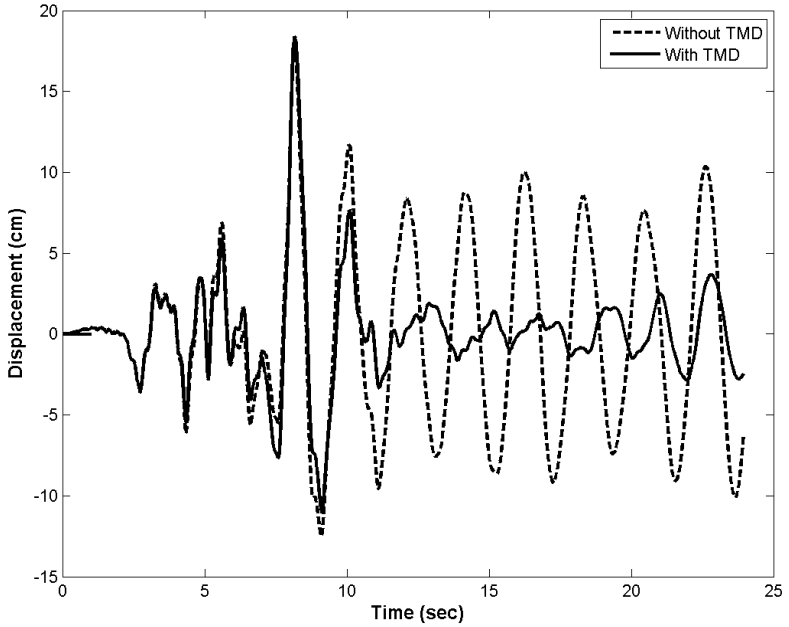

Fig. 6. Displacement Results for the Roof of a First Floor Irregular Structure Subjected to the Northridge Earthquake (PGA = 0.1g)

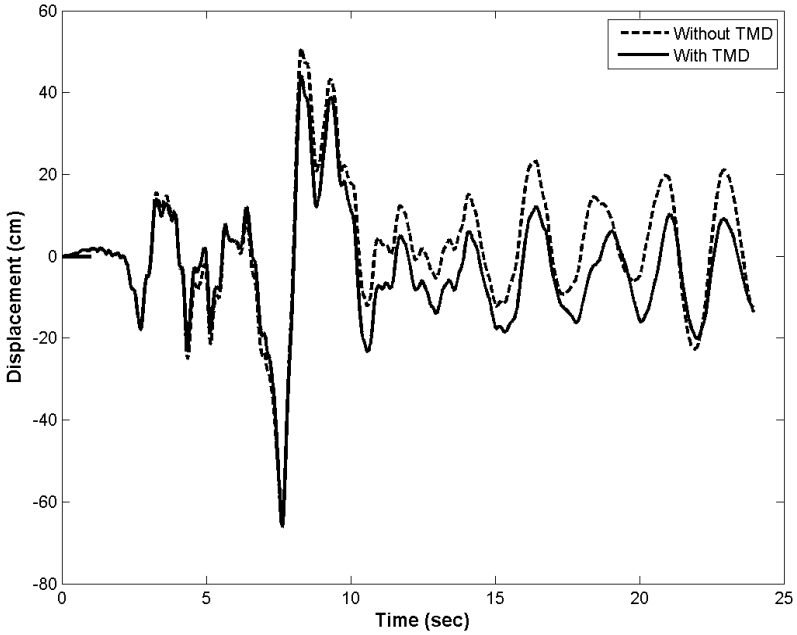

Fig. 7. Displacement Results for the Roof of a First Floor Irregular Structure Subjected to the Northridge Earthquake (PGA = 0.5g).

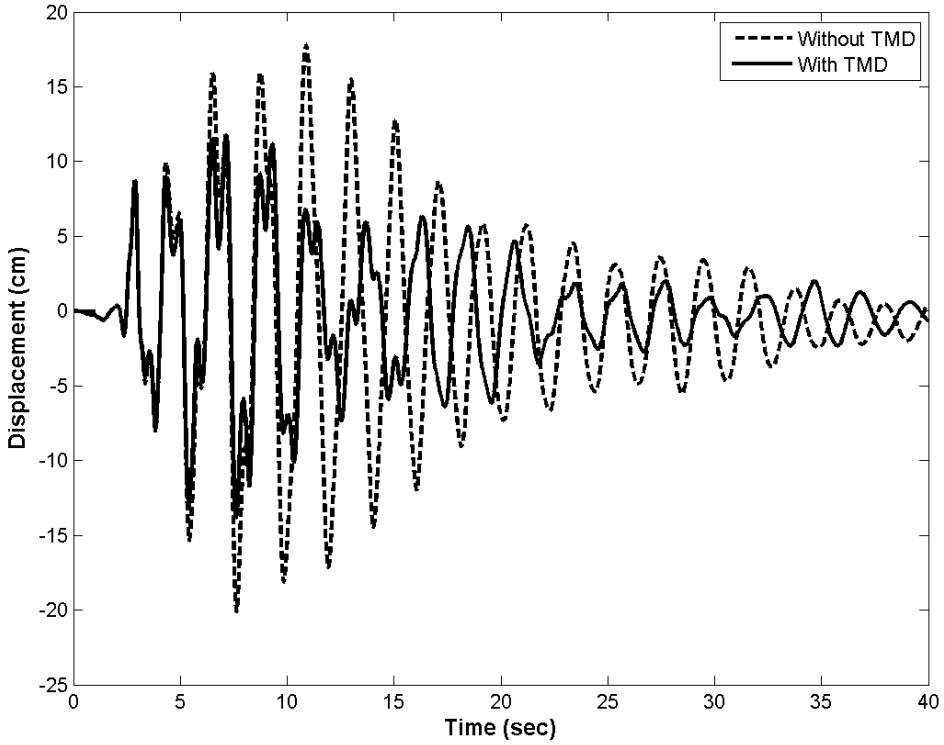

Fig. 8. Displacement Results for the Roof of a First Floor Irregular Structure Subjected to the Loma Prieta Earthquake (PGA = 0.1g).

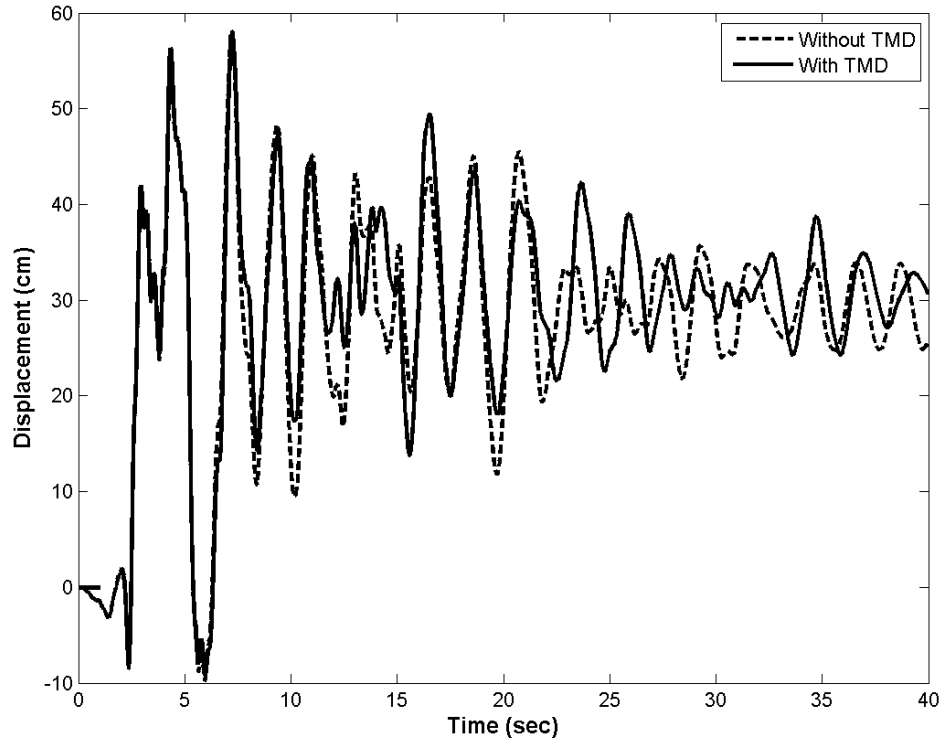

Fig. 9. Displacement Results for the Roof of a First Floor Irregular Structure Subjected to the Loma Prieta Earthquake (PGA = 0.1g).

Table 3.
Average Value of the Max Displacement and RMS of the Roof of an Irregular Mass Structure, on the first floor, based on Far-Field Earthquakes.

PGA (g)	Maximum Displacement Without TMD (m)	Maximum Displacement With TMD (m)	Improvement Percentage (%)	RMS Displacement Without TMD	RMS Displacement With TMD	Improvement Percentage (%)
0.1	0.173445	0.145972	15.83991	0.057023	0.040513	28.9532
0.2	0.302264	0.284084	6.014618	0.089495	0.078165	12.66056
0.3	0.439324	0.41489	5.561635	0.145609	0.12569	13.6795
0.4	0.562072	0.527158	6.211637	0.198112	0.180278	9.002074
0.5	0.686354	0.664339	3.20761	0.255903	0.240394	6.06052
0.6	0.872908	0.838559	3.934994	0.318703	0.297711	6.586894
0.7	1.042032	0.993992	4.610225	0.388044	0.357605	7.844112
0.8	1.175709	1.124033	4.395306	0.476212	0.445622	6.423667
0.9	1.296003	1.2515	3.433812	0.590326	0.566301	4.069801
1	1.52912	1.458938	4.589753	0.759828	0.731229	3.763871

Table 4.
Average Value of the Max Displacement and RMS of the Roof of an Irregular Mass Structure, on the first floor, based on Near-Field Earthquakes.

PGA (g)	Maximum Displacement Without TMD (m)	Maximum Displacement With TMD (m)	Improvement Percentage (%)	RMS Displacement Without TMD	RMS Displacement With TMD	Improvement Percentage (%)
0.1	0.175082	0.153607	12.26566	0.069406	0.047976	30.8761
0.2	0.292425	0.26969	7.774757	0.102512	0.084152	17.90967
0.3	0.365223	0.361781	0.94262	0.127997	0.116961	8.621934
0.4	0.4678	0.454979	2.740877	0.181596	0.169954	6.410901
0.5	0.63562	0.608407	4.281329	0.268648	0.256543	4.505683
0.6	0.817389	0.788752	3.503432	0.37783	0.367164	2.823026
0.7	0.989052	0.96579	2.351916	0.500902	0.491206	1.935773
0.8	1.178935	1.186076	-0.60574	0.620533	0.62237	-0.29599
0.9	1.444845	1.435195	0.667892	0.78168	0.78257	-0.11387
1	1.747475	1.737858	0.550318	0.990577	0.979613	1.106911

Table 5.
Average Maximum value and RMS of Base Stress and of the Roof of an Irregular Mass Structure, on the first floor, based on Far-Field Earthquakes.

PGA (g)	Maximum Shear Without TMD (N)	Maximum Shear With TMD (N)	Improvement Percentage (%)	RMS Shear Without TMD	RMS Shear With TMD	Improvement Percentage (%)
0.1	120324.6	107876.7	10.34528	31513.37	23932.48	24.05611
0.2	180067.6	179650.6	0.231619	43919.6	38364.42	12.64852
0.3	206397.6	207471	-0.52008	50432.72	47072.67	6.662439
0.4	236802.6	236256.2	0.230771	56852.03	54120.48	4.804667
0.5	258791.5	258414.7	0.145589	62869.46	60253.4	4.161107
0.6	282289.8	282133.3	0.055445	68410.52	66070.33	3.420809
0.7	302129.6	302778	-0.21462	73784.92	71641.11	2.905494

0.8	320046.6	320900.9	-0.26693	78856.89	76955.83	2.41078
0.9	337532.7	337875	-0.10141	83787.88	82063.91	2.057536
1	353891.7	354025.9	-0.03791	88432.58	86947.71	1.679093

Table 6.
Average Maximum value and RMS of Base Stress and of the Roof of an Irregular Mass Structure, on the first floor, based on Near-Field Earthquakes.

PGA (g)	Maximum Shear Without TMD (N)	Maximum Shear With TMD (N)	Improvement Percentage (%)	RMS Shear Without TMD	RMS Shear With TMD	Improvement Percentage (%)
0.1	119752.3	108133.2	9.702601	39954.3	30959.3	22.51322
0.2	181544.8	177540.7	2.205563	53019.22	47611.95	10.1987
0.3	224524.2	221521.6	1.337302	59827.78	56356.37	5.802328
0.4	251806.4	252344.9	-0.21385	66138.34	64281.66	2.807273
0.5	268535.8	268888.3	-0.1313	73329.64	71929.59	1.909258
0.6	284797.8	283564.2	0.433179	80625.29	79463.19	1.441354
0.7	307781.5	302989	1.557111	87715.01	86700.26	1.156868
0.8	328393.7	324688	1.128422	94440.58	93652.87	0.834084
0.9	345337.2	342769.2	0.743621	100751.8	100126.2	0.620924
1	359041.5	357492	0.431566	106693.4	106235.3	0.429358

6. Conclusions

In this research, the vibration control of structure with irregular masses, subjected to near-field and far-field earthquakes has been optimized using a tuned mass damper. The efficiency of TMDs in reducing the response of the structure when subjected to destructive earthquakes has also been studied. Based on the analyses performed on the effect of various earthquakes on regular structures with and without dampers, it can be confirmed that mass dampers can be beneficial in any type of earthquake, the results of which are presented in the form of structural averages. Thus, the conclusion of this study can be described as follows:

TMDs in structures with mass irregularities show a better performance in floors 1 to 5, compared to the first and fifth floor. By creating mass irregularities in the stories, structures become more prone to damage in near-field earthquakes compared to far-field earthquakes.

The performance of TMD when subjected to far-field earthquakes is better than near-field earthquakes. Additionally, despite their ineffectiveness in reducing the maximum structural response, TMDs prove to be very useful in reducing vibrations during the earthquake application time and results variance is lower in structures with tuned mass dampers.

References

1. Frahm, H., *Device for damping vibrations of bodies*. 1911, Patent.

2. Wirsching, P.H. and J.T. Yao, *Safety design concepts for seismic structures.* Computers & structures, 1973. **3**(4): p. 809-826.

3. Mashkat Razavi, H., *Intelligent algorithms in structural control with tuned mass dampers considering soil-structure interaction*. 2016, PhD Dissertation, University of Mashhad, December, 2014 (In Persian). Modares Civil Engineering Journal (MCEJ) Vol. 16.

4. Dong, R.G., *Vibration-absorber effect under seismic excitation.* Journal of the Structural Division, 1976. **102**(10): p. 2021-2031.

5. Ohno, S., *Optimum tuning of the dynamic damper to control response of structures to earthquake ground motion.* Proc. 6WCEE, 1977, 1977.

6. Randall, S., D. Halsted, and D. Taylor, *Optimum vibration absorbers for linear damped systems.* Journal of Mechanical Design, 1981. **103**(4): p. 908-913.

7. Pirizadeh, M. and H. Shakib, *Probabilistic seismic performance evaluation of non-geometric vertically irregular steel buildings.* Journal of Constructional Steel Research, 2013. **82**: p. 88-98.

8. Sanaei, E. and M. Babaei, *Topology optimization of structures using cellular automata with constant strain triangles.* International Journal of Civil Engineering, 2012. **10**(3): p. 179-188.

9. Babaei, M., J. Dadash Amiri, F. Omidi, A. Memarian, *Optimal Topologies for Steel Frames with Ordinary Chevron and X-Braces: The Effect on Total Structural Cost.* The Open Civil Engineering Journal, 2016. **10**(1).

10. Babaei, M., *Multi-objective Optimal Number and Location for Steel Outrigger-belt Truss System.* Journal of Engineering Science and Technology, 2017. **12**(10): p. 2599-2612.

11. Babaei, M. and E. Sanaei, *Multi-objective optimal design of braced frames using hybrid genetic and ant colony optimization.* Frontiers of Structural and Civil Engineering, 2016. **10**(4): p. 472-480.

12. Building and Housing Research Center, *Standard No. 2800 "Iranian Code of Practice for Seismic Resistant Design of Buildings", Third Revision, Building and Housing Research Center, Tehran*. 2005.

13. Code, I.N.B., *Part 6: Applied loads on buildings*. 2013, Iranian National Building Code, Tehran, Iran.

14. Krawinkler, H., *Shear in beam-column joints in seismic design of steel frames.* Engineering Journal, 1978. **15**(3).

15. Pastia, C. and S.-G. Luca, *Vibration control of a frame structure using semi-active tuned mass damper.* Buletinul Institutului Politehnic din lasi. Sectia Constructii, Arhitectura, 2013. **59**(4): p. 31.

16. Federal Emergency Management Agency, *National Earthquake Hazards Reduction Program (NEHRP) recommended provisions for seismic regulations for new buildings and other structures*. 2001, Building Seismic Safety Council, United States.